Astron. Nachr./AN **324**, No. 5, 419–424 (2003) / **DOI** 10.1002/asna.200310159

Astrometric detection of binary companions and planets: Acceleration of proper motion

G.H. KAPLAN[1] and V.V. MAKAROV[1,2]

[1] U.S. Naval Observatory, Washington, DC 20392, USA
[2] Universities Space Research Association, Washington, DC 20036, USA

Received 6 January 2003; accepted 19 May 2003; published online 14 July 2003

Abstract. Apparent acceleration of proper motion is one of the observable manifestations of orbital motion in binary stars. Owing to the increasing accuracy of astrometric measurements, it may also be a method to detect binarity of stars. This paper presents some analytical expressions for the effects of binary motion on proper motions when the orbital period is at least several times the span of observations. We estimate orbit dimensions and distances at which low-mass companions and planets may be detected around main-sequence stars, using preliminary estimates of precision for the AMEX, GAIA and SIM space missions.

Key words: astrometry – binaries: general – planetary systems – catalogs

1. Introduction

The publication of the Hipparcos catalog (ESA 1997) has drawn new attention to the problem of the determination of proper motions of stars that are components of binary or multiple systems. With only 3 years of observational data, it was recognized that unmodeled binary motion could affect the proper motions of many stars in the Hipparcos catalog. Most of the concern has been with binaries without known orbits that may have periods of several years to several decades. Yet half of solar-type binary systems have semimajor axes of 50 AU or more, implying, for solar-mass components, periods of a century or more (Duquennoy & Mayor 1991). Such systems can create problems when observational catalogs made years or decades apart are combined (as in Tycho 2) in an effort to provide improved proper motions. Thus, the binary-motion problem occurs on many time scales and may affect, to some degree, a significant fraction of the data in compiled catalogs.

On the other hand, apparent accelerations prove to be a powerful instrument in discovering new binary systems. The short-term Hipparcos proper motions may be compared with long-term ground-based proper motions (e.g., from FK5), and new binaries with a significant orbital motion can be revealed even if the companion is invisible or unresolved. Wielen et al. (1999) developed a model that estimates the statistical significance of such differences, and pointed out that with particularly long and accurate series of observations, it may be possible to estimate the period and, furthermore, the mass of the companion. Nonlinear motion of photocenters of a few hundred suspected binaries was in fact estimated by Gontcharov et al. (2001) from a collection of ground-based catalogs and Hipparcos.

In this paper we assume that no information is available for an astrometric analysis of proper motions other than the data obtained with a short-term space mission. We investigate stellar paths that are almost, but not quite, linear. This case has received less attention than astrometric orbital solutions, although Eisner & Kulkarni (2001) presented an earlier analysis. We provide a simplified model of astrometric observation analysis to quantify the problem. We use the results to estimate the range of detectable orbits for small brown dwarf and Jupiter-mass companions, for three planned space missions, GAIA, SIM and the joint American-German project AMEX.

2. Detectability of brown dwarfs and planets

The inequality B3, derived in Appendix B, is used to estimate the distances and orbits of very small brown dwarfs ($0.01 M_{\odot}$) and Jupiter-mass planets ($0.001 M_{\odot}$) around main sequence dwarfs that could be detected via the acceleration method with the AMEX, GAIA and SIM space astrometry satellites. The minimum detectable semimajor axis with this method is defined by the constraint $2T < P$, where T is the total duration of a mission, and P is the orbital period. Since

Correspondence to: G. Kaplan, gkaplan@usno.navy.mil

 0004-6337/03/0507-0419 $ 17.50+.50/0

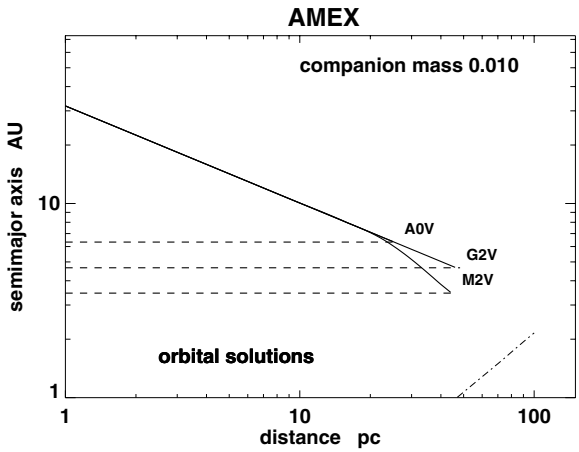

Fig. 1. Detectable orbits of a $0.01 M_{\odot}$ companion (brown dwarf).

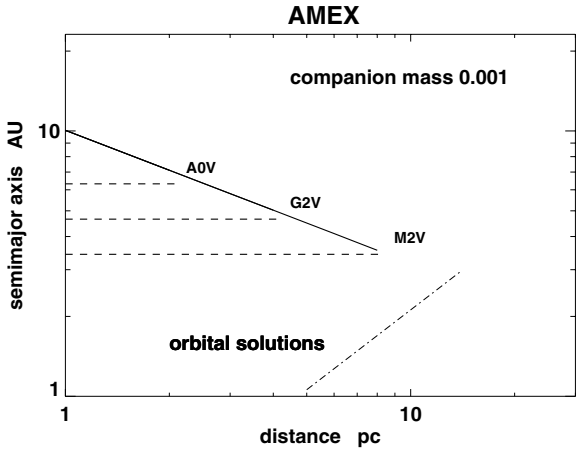

Fig. 2. Detectable orbits of a $0.001 M_{\odot}$ companion (a Jupiter).

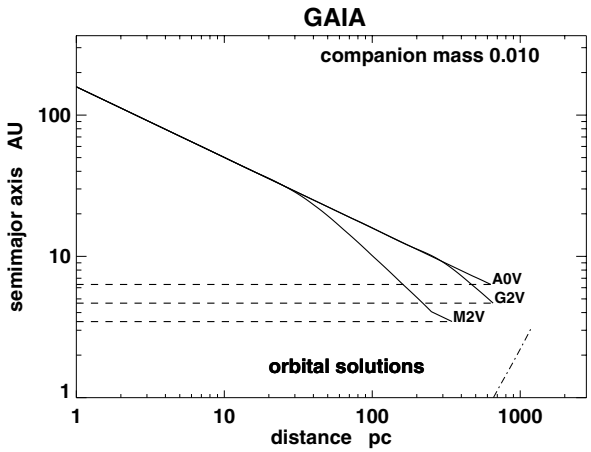

Fig. 3. Detectable orbits of a $0.01 M_{\odot}$ companion (brown dwarf).

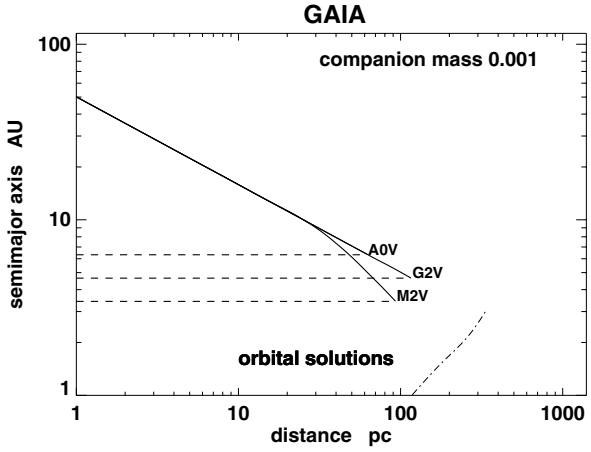

Fig. 4. Detectable orbits of a $0.001 M_{\odot}$ companion (a Jupiter).

the mission length of all three missions is 5 years, the $a_{\min}$ is the same irrespective of the distance to the object, namely, 3.4, 4.7 and 6.3 AU for a M2V, G2V and A0V host, respectively. A single Jupiter around a Sun-like star, therefore, can be detected by any of the satellites at appropriate distances (in the Solar system, $a_{\rm Jupiter} = 5.2028$ AU).

The triangular shapes in Figs. 1 to 5 show the domains of detectable brown dwarf and Jupiter-mass companions, using acceleration solutions, for the three missions in question. The detection domains of orbit solutions lie below these triangles. We assumed the mission-average accuracy measure ϵ in Eq. B3 to be twice the expected sky-average 1σ accuracy of parallaxes, taken from the NASA SMEX proposal for AMEX, (ESA-SCI(2000)4) for GAIA, and (Unwin 2000) for SIM. The upper limit $a_{\max}$ for SIM is magnitude- and spectral type-independent, since with this pointing mission, the nominal accuracy of parallaxes ($\approx$ 1 μas) can be achieved by picking suitable exposure times. As mentioned in Appendix A, the calculated upper detectability limits approximately correspond to the 95% confidence level; therefore, the smallest detected accelerations will have a probability of 0.95. Such moderately reliable detections are of interest for the AMEX mission that would precede the more accurate pointing SIM mission and select suitable targets for planet detection. The upper limit of detection at a 99% confidence is ≈ 1.2 times lower in a than the boundaries in Figs. 1-5.

The figures also show the approximate lower limits of detectable semimajor axes for orbit solutions, although such solutions are not considered in detail in this paper. The thin dot-dashed lines in Figs. 1-5 indicate the lower limit of approximate 95%-confidence detection domains for G2V primary stars with orbital solutions. It is obtained from the simple requirement that the average astrometric excursion should be larger than $\epsilon/0.87$ (cf. Appendix 2; 0.87 is an average projection factor). Thus, at a given distance, and for a given primary and companion mass, the astrometric sensitivity increases with semimajor axis, provided at least one full period is observed. However, once only a fraction of a period can be observed, the astrometric sensitivity decreases with increasing semimajor axis, because the observed motion becomes more linear. As the distance increases, the width of the regime of detectable semimajor axes narrows, since the observational scatter corresponds to an increasing linear scale. Thus there is a reduced range of semimajor axes that are greater than the scatter but less than that for which the orbital motion is statistically indistinguishable from a straight line.

Eisner & Kulkarni (2001) investigated the long-period regime from a different perspective, examining how the pa-

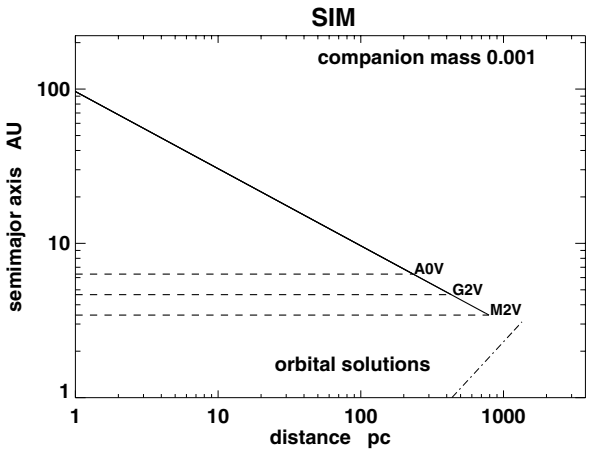

Fig. 5. Detectable orbits of a $0.001 M_\odot$ companion (a Jupiter).

rameters for a simple orbital fit evolve as the period increases beyond the span of the observations. They considered several cases of circular orbits with known inclinations; the analysis in our paper corresponds most closely to what Eisner & Kulkarni would call "type II errors" for either face-on or inclined orbits. From geometric considerations, they obtain a measure of the signal amplitude required for detection (their eq. 25) that is quadratic in P/T for $P >> T$, where P is the orbital period and T is the time span of the observations. A little algebra shows that our upper limit for the semimajor axis, a, in eq. B3, which is proportional to $T/\sqrt{\text{distance}}$, is consistent with an astrometric signature that must increase as $(P/T)^2$ for detection (all other things being equal). Eisner & Kulkarni test their analytic formulas with numerical simulations. For the face-on and inclined circular orbits their simulation results (their Figs. 6 and 9) actually seem to indicate a required amplitude that increases approximately as $(P/T)^{1.9}$. It is unclear to what extent this somewhat more optimistic result is affected by the fact that they apparently did not solve for the period (curvature) of the orbits that they generated.

3. Conclusions

AMEX will be able to detect curved paths of solar-type stars (G2V) due to the presence of a low-mass brown dwarf out to distances ≈ 50 pc. This spectral type is optimal for a search of binary brown dwarfs with AMEX. The range of detectable orbits at $d = 10$ pc is 5 to 10 AU. AMEX will be able, in principle, detect the influence of Jupiter-mass planets around G2V stars out to ≈ 4 pc, and out to ≈ 8 pc around M2V stars, but the range of orbit sizes is fairly small at $d = 4$ pc, 3 to 4 AU. The actual prospect of such detections are defined by the rate of jupiters in the immediate Solar neighborhood.

GAIA will improve on the detectability limits roughly a factor of 15. Brown dwarfs at low orbits will be detectable out to distances ≈ 700 pc, and jupiters to ≈ 100 pc, for solar-type stars. Conversely, these objects may generate difficulties in the data reduction, requiring more complex models. The rate of acceleration detection will grow at least a factor 3300, with respect to AMEX. Quist (2001) conducted extensive simulations of the detectability rates of binary stars for GAIA, using a Galaxy model and provisional data reduction models. It follows from his simulations, that more than half of all $0.01 M_\odot$ companions around stars brighter than M2V with periods between 15 and 40 years will be safely detected with GAIA (confidence 99.87%). The cubic model, that includes also the second derivative of proper motion, can sometimes detect more companions at smaller orbital periods, than the quadratic model considered in this paper, but it is practically useless, since at these smaller periods, the orbital model will always have a higher detection rate.

SIM will have moderate chances to detect Jupiter-mass planets around late-type dwarfs out to distances ≈ 700 pc, and excellent chances out to ≈ 200 pc. But since there are perhaps a hundred million M dwarfs within 1 kpc, SIM will be able to observe only a tiny fraction of them. A precursor, survey-type mission is therefore desirable, that would help to select the most promising targets.

References

Bevington, P.R., Robinson, D.K.: 1992, *Data Reduction and Error Analysis for the Physical Sciences*, McGraw-Hill, New York
Duquennoy, A., Mayor, M.: 1991, A&A 248, 485
Eisner, J.A., Kulkarni, S.R.: 2001, ApJ 561, 1107
ESA: 1997, *The Hipparcos and Tycho Catalogues*, ESA SP-1200
ESA: 2000, *GAIA – Composition, Formation and Evolution of the Galaxy*, ESA Concept and Technology Study Report (ESA–SCI (2000)4)
Gontcharov, G.A., Andronova, A.A., Titov, O.A., Kornilov, E.V.: 2001, A&A 365, 222
Kaplan, G.H.: 2002, Curved Stellar Paths and Proper Motion Determination, unpublished technical report, http://aa.usno.navy.mil/kaplan/curvpath.ps
Quist, C.F.: 2001, A&A 370, 672
Wielen, R., Dettbarn, C., Jahreiß, H., Lenhardt, H., Schwan, H.: 1999, A&A 346, 675
Unwin, S.: 2000, in: J. Bergeron, A. Renzini (eds.), Proc. of the ESO Symp. *From Extrasolar Planets to Cosmology: The VLT Opening Symposium*, Springer-Verlag, Berlin, p. 492

Appendix A: Simplified development of proper motion estimation

In this section we develop a simple model of how analysis of astrometric observations for stellar proper motion determination can become contaminated by an unmodeled acceleration. The objective is to provide approximate expressions that will allow us to determine the order of magnitude of the effect as well as its qualitative nature.

The equation of motion of a body can be expressed as a Taylor series in vector form as

$$\bar{\mathrm{P}}(t) = \bar{\mathrm{P}}_0 + \bar{\mathrm{V}}_0 t + \tfrac{1}{2}\bar{\mathrm{Z}} t^2 + \cdots \quad \text{(A1)}$$

where $\bar{\mathrm{P}}_0$ and $\bar{\mathrm{V}}_0$ are the body's position and velocity at time $t = 0$, and $\bar{\mathrm{Z}}$ is the acceleration. For a star where the acceleration is due to the gravitational attraction of a companion (either seen or unseen), $\bar{\mathrm{Z}} = (GM/R^2)\hat{R}$, where G is the constant of gravitation and M and R are the mass and

distance of the companion. The unit vector $\hat{R}$ points toward the companion. If we assume a constant acceleration — i.e., truncate eq. A1 after the third term — we are limited to considering a small segment of the orbit. This is the problem we wish to investigate: the parabolic approximation constitutes a "weak curvature" case.

Let the star's motion, projected onto the plane of the sky, be $\bar{\mathrm{p}}(t)$. The plane of the sky is orthogonal to the line of sight unit vector $\hat{\mathrm{n}}$, so we have

$$\begin{aligned}\bar{\mathrm{p}}(t) &= \bar{\mathrm{P}}(t) - (\bar{\mathrm{P}}(t)\cdot\hat{\mathrm{n}})\hat{\mathrm{n}}\\ &= (\bar{\mathrm{P}}_0 + \bar{\mathrm{V}}_0 t + \tfrac{1}{2}\bar{\mathrm{Z}}t^2) - ((\bar{\mathrm{P}}_0 + \bar{\mathrm{V}}_0 t + \tfrac{1}{2}\bar{\mathrm{Z}}t^2)\cdot\hat{\mathrm{n}})\hat{\mathrm{n}}\\ &= \bar{\mathrm{P}}_0 + \bar{\mathrm{V}}_0 t + \tfrac{1}{2}\bar{\mathrm{Z}}t^2 - (\bar{\mathrm{P}}_0\cdot\hat{\mathrm{n}})\hat{\mathrm{n}} - (\bar{\mathrm{V}}_0\cdot\hat{\mathrm{n}})t\hat{\mathrm{n}}\\ &\quad -\tfrac{1}{2}(\bar{\mathrm{Z}}\cdot\hat{\mathrm{n}})\ t^2\hat{\mathrm{n}}\\ &= [\bar{\mathrm{P}}_0 - (\bar{\mathrm{P}}_0\cdot\hat{\mathrm{n}})\hat{\mathrm{n}}] + [\bar{\mathrm{V}}_0 - (\bar{\mathrm{V}}_0\cdot\hat{\mathrm{n}})\hat{\mathrm{n}}]t\\ &\quad +\tfrac{1}{2}[\bar{\mathrm{Z}} - (\bar{\mathrm{Z}}\cdot\hat{\mathrm{n}})\hat{\mathrm{n}}]\ t^2 \qquad \text{(A2)}\end{aligned}$$

That is, the star's motion in the plane of the sky can be represented as

$$\bar{\mathrm{p}}(t) = \bar{\mathrm{p}}_0 + \bar{\mathrm{v}}_0 t + \tfrac{1}{2}\bar{\mathrm{z}}\ t^2 \qquad \text{(A3)}$$

where $\bar{\mathrm{p}}_0$ is $\bar{\mathrm{P}}_0$ projected onto the sky $= \bar{\mathrm{P}}_0 - (\bar{\mathrm{P}}_0\cdot\hat{\mathrm{n}})\hat{\mathrm{n}}$
$\bar{\mathrm{v}}_0$ is $\bar{\mathrm{V}}_0$ projected onto the sky $= \bar{\mathrm{V}}_0 - (\bar{\mathrm{V}}_0\cdot\hat{\mathrm{n}})\hat{\mathrm{n}}$
$\bar{\mathrm{z}}$ is $\bar{\mathrm{Z}}$ projected onto the sky $= \bar{\mathrm{Z}} - (\bar{\mathrm{Z}}\cdot\hat{\mathrm{n}})\hat{\mathrm{n}}$

The vectors $\bar{\mathrm{p}}(t)$, $\bar{\mathrm{p}}_0$, $\bar{\mathrm{v}}_0$, and $\bar{\mathrm{z}}$ have no component along the line of sight $\hat{\mathrm{n}}$ and are therefore 2-vectors in a coordinate system on the plane of the sky.

In standard current practice, a star's motion is expressed as $\bar{\mathrm{p}}'(t) = \bar{\mathrm{p}}'_0 + \bar{\mathrm{v}}'t$. Here, $\bar{\mathrm{v}}'$ represents the star's proper motion as conventionally defined — assumed constant, hence without subscript. (In this development we are ignoring terms for the curvature of the sky and are assuming that aberration and parallax have already been removed from the data.) It is tempting to think of eq. A3 as a simple extension of the conventional expression, carried to higher order. But $\bar{\mathrm{v}}_0$ in eq. A3 does not correspond to proper motion. For a gravitationally bound binary, proper motion properly refers to the projection on the sky of the (constant) space velocity of the center of mass of the system. In eq. A3, $\bar{\mathrm{v}}_0$ is the instantaneous linear component of the star's apparent motion, which is the sum of the proper motion of system plus the projected orbital velocity of the star (at t=0) around the center of mass. Determination of the true proper motion of the system would require observations of the star spanning nearly an orbital period, or observations of both the star and its companion over a shorter period together with an estimate of their mass ratio.

But here we wish to consider a series of observations where the orbital motion of the star is not obvious. Consider an observation of the star's position, $\bar{\mathrm{p}}_i$, taken at time t_i, with a measurement error $\bar{\mathrm{e}}_i$ (all vectors are now in the plane of the sky). Then $\bar{\mathrm{p}}_i = \bar{\mathrm{p}}_0 + \bar{\mathrm{v}}_0 t_i + \frac{1}{2}\bar{\mathrm{z}}t_i^2 + \bar{\mathrm{e}}_i$. But if we have no knowledge of the acceleration, we will model the star's motion in the conventional way as $\bar{\mathrm{p}}'(t) = \bar{\mathrm{p}}'_0 + \bar{\mathrm{v}}'t$ (see Fig. A1). The difference between the observation and this incomplete model of the star's motion at time t_i is then

$$\bar{\mathrm{e}}'_i = \bar{\mathrm{p}}_0 + \bar{\mathrm{v}}_0 t_i + \tfrac{1}{2}\bar{\mathrm{z}}t_i^2 + \bar{\mathrm{e}}_i - \bar{\mathrm{p}}'_0 - \bar{\mathrm{v}}'t_i \qquad \text{(A4)}$$

Compared to our incomplete model, the observation will appear to be in error by an amount $\bar{\mathrm{e}}'_i$. This error is the sum of the random error of observation and the systematic error resulting from the use of the incorrect model. Despite the fact that it is not a purely stochastic quantity, it provides a basis for investigating what would happen if the incomplete model were fit to a set of N two-dimensional observations using least squares. Let us take the common situation where the measurement errors $\bar{\mathrm{e}}_i$ are assumed to all have approximately the same magnitude $\langle e\rangle$ and the observations are therefore all given unit weight. In such a case, the quantity that would be minimized is the sum of $\bar{\mathrm{e}}'^2_i$ over all observations. The method would determine the position $\bar{\mathrm{p}}'_0$ (at time t=0) and proper motion $\bar{\mathrm{v}}'$ that minimize $\sum \bar{\mathrm{e}}'^2_i$. The quantities $\bar{\mathrm{p}}'_0$ and $\bar{\mathrm{v}}'$ are not particularly interesting in themselves, but the *differences* between these quantities and the corresponding ones from eq. A3 for this case are key to further analysis. That is, we are interested in $\Delta\bar{\mathrm{p}} = \bar{\mathrm{p}}_0 - \bar{\mathrm{p}}'_0$ and $\Delta\bar{\mathrm{v}} = \bar{\mathrm{v}}_0 - \bar{\mathrm{v}}'$. These quantities measure in some sense the "error" in the position-at-epoch and proper motion derived from the linear fit.

One can perform a standard least-squares analysis of this case, which amounts to the fit of a straight line to a series of observations along a parabola; see Kaplan (2002). We obtain

$$\Delta\bar{\mathrm{p}} = \tfrac{1}{12}\bar{\mathrm{z}}T^2 \qquad \text{and} \qquad \Delta\bar{\mathrm{v}} = -\tfrac{1}{2}\bar{\mathrm{z}}T \qquad \text{(A5)}$$

Since the vectors $\Delta\bar{\mathrm{p}}$, $\Delta\bar{\mathrm{v}}$, and $\bar{\mathrm{z}}$ are collinear, we can dispense with the vector notation and use use the symbols Δp, Δv, and z for the vector magnitudes. Equation A5 then becomes

$$\Delta p = \tfrac{1}{12}zT^2 \qquad \text{and} \qquad \Delta v = -\frac{1}{2}zT \qquad \text{(A6)}$$

The difference between the actual position of the star and that computed from the linear model at time t is in the direction of $\bar{\mathrm{z}}$. The acceleration $\bar{\mathrm{z}}$ is always toward the companion, and for $\bar{\mathrm{z}}$ to be considered essentially constant, the companion must be sufficiently far away that neither its direction nor distance change significantly over the short orbital arc we are considering. The magnitude of the difference between the actual motion and the linear model is

$$\delta = \Delta p + \Delta v t + \tfrac{1}{2}zt^2 = \tfrac{1}{12}zT^2 - \tfrac{1}{2}zTt + \tfrac{1}{2}zt^2 \qquad \text{(A7)}$$

This equation also holds for the individual components of the motion. The function δ has an extremum ($d\delta/dt$=0) at t=$T/2$, in the middle of the span of observations, where $\delta = -zT^2/24$. At the beginning and end of the span of observations (t=0 and t=T), $\delta = zT^2/12$. The total range of δ over the time interval of interest is thus $zT^2/8$. The locus of actual motion of the star on the sky crosses the least-squares-determined straight line where the δ function has zeros, at $t = T/2 \pm \sqrt{T/12} = 0.211T$ and $0.789T$. See Fig. A1.

We will refer to $zT^2/24$, which is the absolute value of δ at $t = T/2$, as the *amplitude of the modeling error* from the linear approximation, designated by h. The total range of δ over the time span of interest is $3h$. In the following developments we will use h as the metric for determining the sensitivity of the N observations to the acceleration. Intuitively, it would seem that if h is a few times $\langle e\rangle/\sqrt{N}$, where $\langle e\rangle$ is the mean error of a single observation (unit weight), then the observations should be at least marginally sensitive

to the acceleration. More precisely, if we compute the ratio of the post-fit sum-of-squares X^2 for the linear and quadratic models, expressed as a function of h, we can use an F-test to determine the significance of the acceleration term.

The post-fit sum-of-squares for the case of the linear fit to accelerated motion is

$$X^2 = N(\tfrac{1}{720} z^2 T^4) + \sum_{i=1}^{N} e_i^2 \tag{A8}$$

Here, the e_i are the lengths of the 2D error vectors, that is, $e_i^2 = \bar{\mathrm{e}}_i \cdot \bar{\mathrm{e}}_i$. But $\langle e \rangle$ is defined such that $\sum_{i=1}^{N} e_i^2 = N\langle e \rangle^2$, so eq. A8 becomes

$$X^2 = N\left(\frac{1}{720} z^2 T^4 + \langle e \rangle^2\right) \tag{A9}$$

and the fractional increase in X^2 (the "extra sum of squares") due to the modeling error from the linear approximation (and assuming no other modeling errors) would be

$$\frac{\Delta X^2}{X^2} = \frac{1}{720}\frac{z^2 T^4}{\langle e \rangle^2} = \left(\frac{1}{26.8}\frac{zT^2}{\langle e \rangle}\right)^2 \approx \left(\frac{h}{\langle e \rangle}\right)^2 \tag{A10}$$

where z and $\langle e \rangle$ are expressed in the same angular units, and h is the previously defined amplitude of the modeling error, $zT^2/24$. Suppose we set $h = g\langle e \rangle/\sqrt{N}$, where g is a factor to be determined; then the fractional increase in X^2 is g^2/N. The ratio F that is subject to the F-test is the fractional increase in X^2 (= fractional increase in χ^2, since all observations have a an uncertainty of $\langle e \rangle$) times the number of degrees of freedom, ν, in the quadratic fit (see, e.g., Bevington & Robinson 1992, eq. 11.50):

$$F = \frac{\Delta X^2}{X^2/\nu} = \frac{g^2}{N}\nu \tag{A11}$$

If N is sufficiently large that $\nu \approx N$, then $F \approx g^2$. For an F-test probability of 95%, F would have to be about 4 for a wide range of degrees of freedom (F=4.17 for ν=30, 3.92 for ν=120, 3.84 for ν=∞). Thus we require $g = 2$, i.e., $h = 2\langle e \rangle/\sqrt{N}$. This result is not surprising, since a 2σ value for a model parameter determined from Gaussian-distributed data has a 95% chance of being significantly different from zero. If we wish a more stringent test, we can always set g=3 (probability > 99%); the value of g can be adjusted according to the acceptable ratio of false positives / false negatives in the results.

Appendix B: Estimating the magnitude of the effect

This section provides an assessment of the magnitude of the unmodeled acceleration effect that may be detected with a given mission-average precision of astrometric measurements. The detectable orbits have apparent loci with a range of curvatures. The development given above treats the statistics of stellar loci at the weak curvature limit — those representing a very small part (a few percent) of a binary orbital period. The strong curvature limit might be plausibly defined by the point at which a reliable orbital solution becomes feasible. That point will be somewhat arbitrarily defined here as being half an orbital period, although preliminary orbital solutions are often formed from observations spanning much less time.

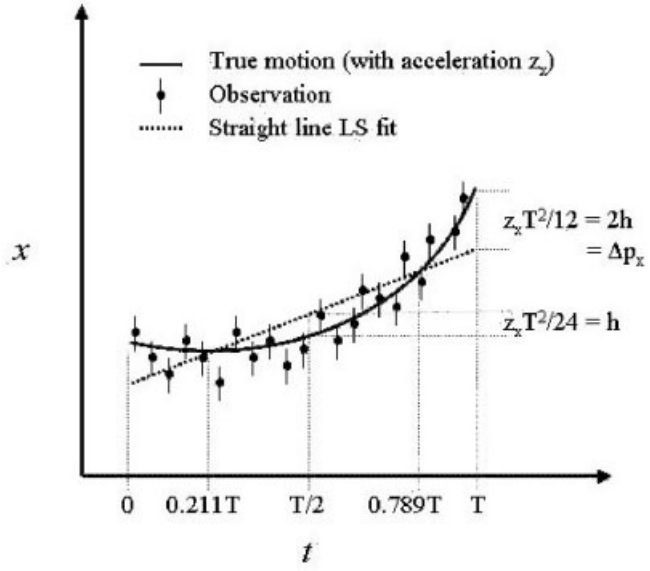

Fig. A1. Representation of a single component of a star's space motion as a function of time. The true, accelerated motion between times 0 and T is indicated by the solid line (the acceleration component is z_x). Observational measurements are indicated that are uniformly distributed in time and normally distributed about the true path of the star. The dashed line is the least-squares straight-line fit to the motion, assuming equally weighted observations. Various parameters of the fit are shown.

To assess the practical effect of unmodeled accelerations, a reasonable approach is to compare, for each candidate binary system, the amplitude of the linear-track modeling error, h, to some detection criterion ϵ that we are free to choose. The results of Appendix A show that a reasonable choice for ϵ is $2\langle e \rangle/\sqrt{N}$, where $\langle e \rangle$ is the mean error of a single observation and N is the number of observations. (More correctly, the denominator should be $\sqrt{\nu}$, where ν is the number of degrees of freedom in the quadratic solution, but we are assuming that N is sufficiently large that $\nu \approx N$.)

The value of the modeling error h is defined for a specific time period of duration T, and we will use the expression $h = zT^2/24$ from Appendix A. Although this expression somewhat underestimates the effect of orbital motion on the data for stars that traverse a significant fraction of their orbits in time T, it is the appropriate expression to use for the weak curvature limit.

Our task, then, is to determine over what range of conditions $h > \epsilon$. Since h is proportional to the star's projected acceleration on the sky, z, we must first relate z to the magnitude of the true acceleration of the star in 3-space, $|\bar{\mathrm{Z}}|$. The true acceleration can be expressed in terms of the physical parameters of the binary system, and we can then use what is known about the distribution of these physical parameters to estimate the frequency of significant acceleration effects on astrometric data.

The magnitude of the acceleration projected onto the plane of the sky is related to the magnitude of the true 3-D

acceleration vector by $z = (\sin\theta)|\bar{Z}|/d$, where θ is the angle between the direction of $\bar{Z}$ and the line of sight, and d is the distance to the star. The parallax, p, is $1/d$, so our $h > \epsilon$ condition becomes

$$\frac{1}{24}\,(\sin\theta)\,|\bar{Z}|\,T^2\,p > \epsilon \tag{B1}$$

The acceleration magnitude is related to the physical state of the binary system through $|\bar{Z}| = GM/R^2$, where R is the instantaneous distance between components, and M is either (a) the mass of the companion, if the star's motion is measured in an inertial system, or (b) the total mass of the system, if the motion is measured with respect to the companion. If we use units of AU, years, and solar masses, the gravitational constant $G = 4\pi^2$ and the true acceleration $|\bar{Z}|$ is expressed in AU year^{-2}. If d is in parsecs and p in arcseconds, then z is in units of arcsec year^{-2} and h is in arcsec.

The distance R is obviously closely related to the semimajor axis of the orbit, a. If we write $R = a(R/a)$ (for reasons that will become apparent shortly) our condition for detection of weak curvatures becomes

$$\frac{4\pi^2\,(\sin\theta)\,M\,T^2\,p}{24\left[a\left(\frac{R}{a}\right)\right]^2} > \epsilon \tag{B2}$$

The strong curvature limit is defined by $P \geq 2T$, where P is the orbital period, given by $P = a^{3/2}/\sqrt{M}$, where M is the total mass of the system. For this limit we therefore have the condition $a^{3/2}/\sqrt{M} > 2T$. Rearranging the expressions for the weak and strong curvature limits, we obtain the limits on the semimajor axis that define the fraction of stars of interest:

$$(2T)^{2/3}\,M^{1/3} \;<\; a \;<\; \frac{\pi T}{\left(\frac{R}{a}\right)}\left(\frac{M\sin\theta}{6}\right)^{1/2}\left(\frac{p}{\epsilon}\right)^{1/2} \tag{B3}$$

Note that M on the left and right sides can have different meanings: on the left it is always the total mass of the system; on the right it is the total mass of the system only if the motion of the star is measured with respect to its companion. If the star's motion is measured with respect to an inertial frame, then M on the right is the mass of the companion. The expressions therefore can be used for investigating planet detection by the astrometric method, in the long-period limit, simply by setting M on the right side to be the planet's presumed mass.

We have chosen $\epsilon = 2\langle e\rangle/\sqrt{N}$, which is twice the 1σ uncertainty of any angular variable derived from the observations (assuming $N \approx \nu$). Therefore, the quantity p/ϵ appearing on the right side of eq. B3 can be thought of as half the signal-to-noise ratio of the parallax: $p/\epsilon = \frac{1}{2}p/\sigma_p$. (This holds only for the case where the parallax of the star is determined using the same set of observations used for the proper motion and acceleration determination.) If we fix the p/σ_p ratio, eq. B3 provides the semimajor axis limits for stars in a certain distance shell; for example, if we wish to consider stars with parallaxes good to 10% ($p/\sigma_p = 10$) when $\sigma_p \approx 10^{-3}$ arcsec, we will obtain the limits on a for stars at a distance of approximately 100 pc. It is interesting to note in this regard that if we have a parallax-limited sample of stars uniformly distributed through space, the average parallax is only 1.5 times the minimum parallax. In such a case, and assuming that the minimum parallax is σ_p, then $p/\epsilon < 1$ for most stars in the sample, and the upper limit on a will generally be quite restricted. However, most catalogs are magnitude-limited and their stellar distributions are much more concentrated toward the Sun. In such catalogs, and in special samples of nearby stars, there will be enough stars with $p/\epsilon > 1$ to provide a useful range of detectable semimajor axes.

To assess quantitatively how many stars fall between the limits defined by eq. B3, we need to know something about the distributions of $\sin\theta$, a, M, and R/a. Two of the four distributions, for $\sin\theta$ and R/a, are easy to deal with. Although the projection factor $\sqrt{\sin\theta}$ is unknown for any specific binary system, we can assume that the direction of the vector separating the two components is randomly distributed over 4π steradians. For such a distribution, the average projection factor is 0.87, the median projection is 0.71. Therefore we can adopt 0.87 as the average value of the projection factor $\sqrt{\sin\theta}$, with some confidence that the average is also typical.

The distribution of R/a values presents a similar situation. For circular orbits, R/a=1 at all times. For stars in eccentric orbits, R/a varies between 1–e and 1+e, where e is the orbital eccentricity. However, binary stars spend more time near apastron than periastron, and over an orbital period the average value of R/a is $1+\frac{1}{2}e^2$. Since this ratio can only take on values between 1 and 1.5, we can adopt an average value of R/a of 1.3 without much concern about the distribution of eccentricities.

Inserting the appropriate numerical quantities, eq. B3 becomes

$$1.59\,T^{2/3}\,M^{1/3} \;<\; a \;<\; 0.86\,T\left(M\,\frac{p}{\epsilon}\right)^{1/2} \tag{B4}$$

Since $\epsilon = 2\sigma_p$, the right side (upper limit to a) could also be expressed as $0.61T(M\,p/\sigma_p)^{1/2}$. As we expect, the range of applicable a increases with T. For $M = 1$ and $p/\epsilon = 1$, $7.4 \leq a \leq 8.7$ if $T = 10$ and $34 \leq a \leq 87$ for $T = 100$. These limits define the null set for $T < 6.1$ years for solar-mass binaries where the parallax is at the limit of detection, but do not preclude more massive or closer systems.